IMAGE SEGMENTATION BY A ROBUST GENERALIZED FUZZY C-MEANS ALGORITHM

Hui Zhang[1,2], *Q. M. Jonathan Wu*[1], *Thanh Minh Nguyen*[1]

[1]Department of Electrical and Computer Engineering, University of Windsor, Canada
[2]School of Computer & Software, Nanjing University of Information Science & Technology, China

ABSTRACT

Fuzzy c-means (FCM) has been considered as an effective algorithm for image segmentation. However, it lacks of sufficient robustness to image noise. In this paper, we propose a simple and effective method to make the traditional FCM more robust to noise, with the help of generalized mean. Traditional FCM can be considered as a linear combination of membership and distance (function) from the expression of its mathematical formula. The proposed generalized FCM (GFCM) is generated by applying generalized mean on these two items. We impose generalized mean on membership to incorporate local spatial information and cluster information, and on distance function to incorporate local spatial information and observation information (image intensity value). Thus, our GFCM is more robust to image noise with the spatial constraints: the generalized mean. The performance of our proposed algorithm, compared with state-of-the-art technologies including modified FCM, HMRF and their hybrid models, demonstrates its improved robustness and effectiveness.

Index Terms—Fuzzy C-Means, Generalized Mean, Image segmentation, Spatial constraints

1. INTRODUCTION

Image segmentation is one of the most important and difficult problems in many applications, such as robot vision, object recognition and medical image processing. Although different methodologies [1-4] have been proposed for image segmentation, it remains a challenge due to overlapping intensities, low contrast of images, and noise perturbation. In the last decades, fuzzy segmentation methodologies, and especially the fuzzy c-means algorithms (FCM) [6], have been widely studied and successfully applied in image clustering and segmentation. Their fuzzy nature makes the clustering procedure able to retain more original image information than the crisp or hard clustering methodologies [5, 7].

Although the FCM algorithm usually performs well with non-noise images, it is still weak in imaging noise, outliers and other imaging artifacts. To overcome this shortcoming, a wide variety of approaches have been proposed to incorporate spatial information in the image [8, 9]. A common approach is the use of a Markov Random Field (MRF) [10]. Such methods aim to impose spatial smoothness constraints on the image pixel labels. Recently, a special case of the MRF model—the Hidden MRF (HMRF) Model—has been proposed [11, 12]. In the HMRF model, the spatial information in an image is encoded through contextual constraints of neighboring pixels, which are characterized with conditional MRF distributions. Based on this well-known approximation, various HMRF model estimation approaches have been proposed.

In this paper, we incorporate generalized mean into FCM, called GFCM, which selects mean template as the spatial constraint. Different from the HMRF model, our model is fully free of the empirically adjusted parameter β. Moreover, HMRF model is computationally expensive to implement. However, our algorithm is easy, simple and fast for implementation. Finally, our algorithm focuses on standard FCM. However, the idea of incorporating generalized mean into FCM can also be easily extended to improve the performance of other FCM-like algorithms, which are modified by adding some type of penalty terms to the original FCM objective function.

2. MATHEMATICAL BACKGROUND

2.1. Generalized mean

In mathematics, a generalized mean, also known as power mean or Hölder mean, is an abstraction of the Pythagorean means including arithmetic, geometric, and harmonic means. The generalized mean of $a_1, a_2, \ldots, a_n$ is defined as

$$M_p\left(a_1, a_2, ..., a_n\right) = \left(\frac{1}{n}\sum_{i=1}^{n} a_i^p\right)^{1/p}, \quad (1)$$

where $a_i \geq 0$, $p \in \left[-\infty, +\infty\right]$.

For $p \to 0$, (1) approaches the geometric mean

$$M_G\left(a_1, a_2, ..., a_n\right) = \left(\prod_{i=1}^{n} a_i\right)^{1/n}. \quad (2)$$

For p=1, (1) results in the arithmetic mean

$$M_A\left(a_1, a_2, ..., a_n\right) = \frac{1}{n}\sum_{i=1}^{n} a_i. \quad (3)$$

2.2. Fuzzy c-means algorithm

To deal with the problem of clustering N multivariate data points into J clusters, Dunn [13] introduced and later Bezdek [6] extended the fuzzy c-means clustering algorithm. In the standard FCM algorithm, the fuzzy objective function that needs to be minimized is given by

$$J_m = \sum_{i=1}^{N}\sum_{j=1}^{J} u_{ij}^m d_{ij} = \sum_{i=1}^{N}\sum_{j=1}^{J} u_{ij}^m \left\| y_i - \mu_j \right\|^2 . \quad (4)$$

where y_i, i=(1,2,…,N), denotes the data set in the D-dimensional vector space, N is the total number of data points, J is the number of clusters, u_{ij} is the degree of membership of y_i in the j-th cluster, m is the weighting exponent on each fuzzy membership function u_{ij}, d_{ij} is a distance (similarity) measure between point y_i and cluster center μ_j, called distance function. The FCM algorithm is iterated through the necessary conditions for minimizing J_m with the following update equations:

$$\mu_j = \frac{\sum_{i=1}^{N} u_{ij}^m y_i}{\sum_{i=1}^{N} u_{ij}^m}, \quad u_{ij} = \frac{\left(d_{ij}\right)^{1/(1-m)}}{\sum_{h=1}^{J}\left(d_{ih}\right)^{1/(1-m)}} . \quad (5)$$

with the constraint $\sum_{j=1}^{J} u_{ij} = 1$.

3. GENERALIZED FUZZY C-MEANS ALGORITHM

Let us first consider (4). It can be easily seen that the objective function is composed of two items: membership u_{ij} and distance function d_{ij}. Our algorithm is simple, easy and straightforward to modify these two items with local generalized mean. This modification incorporates more local spatial information to make the model more robust to image noise. After modification of (1), the local generalized mean is given as

$$M_p = \left(\frac{1}{\mathcal{N}_i} \sum_{c\in\mathcal{N}_i} a_c \right)^{1/p} . \quad (6)$$

where $\mathcal{N}_i$ is the neighborhood of the i-th pixel, including the i-th pixel. It can be easily seen the difference between (global) generalized mean in (1) and local generalized mean in (6). Equation (1) focus on all image pixels i=(1,2,…,N), and (6) focus only on the image pixels m belongs to the neighborhood $\mathcal{N}_i$. Considering weighted factor and local generalized arithmetic mean with distance measure, a new objective function can be given as

$$J_m = \sum_{i=1}^{N}\sum_{j=1}^{J} u_{ij}^m \sum_{c\in\mathcal{N}_i} w_c d_{cj} . \quad (7)$$

where w_c is the weighted factor to control the influence of the neighborhood pixels depending on their distance from the central pixel i. Generally, the strength of w_c should decrease as the distance between pixel c and i increases. By applying the optimization way similar to the standard FCM, the parameters in GFCM can be calculated iteratively as

$$\mu_j = \frac{\sum_{i=1}^{N}\sum_{c\in\mathcal{N}_i} w_c u_{ij}^m y_c}{\sum_{i=1}^{N}\sum_{c\in\mathcal{N}_i} w_c u_{ij}^m} . \qquad u_{ij} = \frac{\left(\sum_{c\in\mathcal{N}_i} w_c d_{cj}\right)^{1/(1-m)}}{\sum_{h=1}^{J}\left(\sum_{c\in\mathcal{N}_i} w_c d_{ch}\right)^{1/(1-m)}} . \quad (8)$$

By applying local weighted generalized mean on membership, the modified membership u_{ij} can be calculated as

$$u_{ij} = \frac{\sum_{c\in\mathcal{N}_i} w_c u_{cj}}{\sum_{h=1}^{J}\sum_{c\in\mathcal{N}_i} w_c u_{ch}} . \quad (9)$$

For a deep understanding of our algorithm, let us give some analysis for usage of generalized mean in detail. Distance function d_{ij} is a measure between point y_i and cluster center μ_j in standard FCM. In our GFCM, this distance is influenced by the distance in its immediate neighborhood to incorporate local spatial information and observation information (image intensity value). The new distance function in our model can be modified as (ignoring constant item)

$$d_{ij} = \sum_{c\in\mathcal{N}_i} w_c \left\| y_c - \mu_j \right\|^2 = \left\| \overline{y}_i - \mu_j \right\|^2 . \quad (10)$$

Here, ||*|| is the squared Euclidean distance which is normally adopted in standard FCM. Equation (10) may explain why our method is more robust to image noise. Assuming image intensity y_i is corrupted by image noise, in this case, calculation of d_{ij} in standard FCM may be far away from the "true" distance function. However, in our model, this distance is calculated by modified $\overline{y}_i$ which is obtained by its immediate neighborhood.

The membership function u_{ij} represents the probability that image pixel i belongs to the cluster j. Similar to distance function, we also use generalized mean to make the membership of image pixel i influenced by the membership in its immediate neighborhood for incorporating local spatial information and cluster information, as shown in (9). That means the probability of i-th pixel belongs to the cluster j is not decided by the pixel i (u_{ij}), but by the neighborhood of pixel i ($\sum_{c\in\mathcal{N}_i} w_c u_{cj}$).

In short, our algorithm is based on an obvious fact. A single image pixel i is easy to be corrupted by noise. However, image pixels in the local neighborhood of i-th pixel are hard to be all corrupted by noise. As long as the "signal" pixels are more than "noise" pixels in this neighborhood, the correct function (membership or distance function) can always be calculated. This is the reason why we use the generalized mean to calculate "average" functions for eliminating the noise effect.

Finally, we summarize the computation process of our algorithm as follows

GFCM Algorithm:

Step 1. Fix the cluster number J, fuzzy membership parameter m and then select initial cluster center.

Step 2. Set the loop counter k=0

Step 3. Update the new cluster center $\mu_j^{(k)}$ using (8).

Step 4. Update the fuzzy membership function $u_{ij}^{(k)}$ using (8) and (9).

Step 5. Terminate the iterations if the object function converges; otherwise, increase the iteration (k=k+1) and repeat steps 2 through 5.

4. EXPERIMENTAL RESULTS AND DISCUSSION

In this section, we experimentally evaluate our proposed GFCM in a set of synthetic images and real images. The neighborhood window size of GFCM is set as 5×5. For simplicity, the weighted factor w_c equals to 1 for all c-th pixels in the neighborhood window. The fuzzy membership weighting is set m=2. We also evaluate GGFCM [2], MFCM [4], FCM_S [5], FLICM [3] and HMRF-FCM [9] for comparison. Our experiments have been developed in Matlab R2009b, and are executed on an Intel Pentium Dual-Core 2.2 GHZ CPU, 2G RAM.

Fig. 1. Original image from the Berkeley image segmentation dataset.

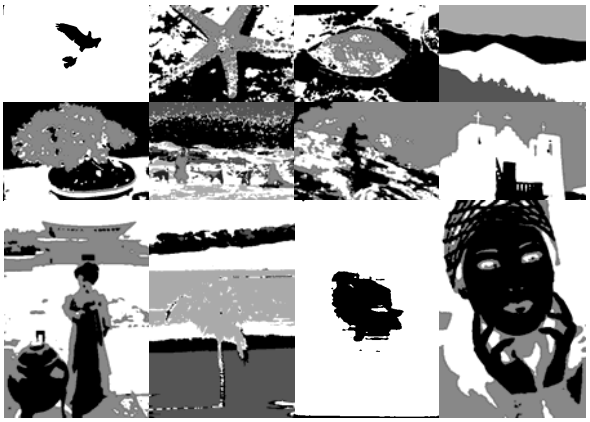

Fig. 2. Image segmentation results by GFCM.

4.1. Real Images

In this experiment, we evaluate the performance of the proposed method based on a subset of the Berkeley image dataset [14], which is comprised of a set of real-world color images along with segmentation maps provided by different individuals. We employ the Probabilistic Rand (PR) index to evaluate the performance of the proposed method, with the multiple ground truths available for each image within the dataset. It has been shown that the PR index possesses the desirable property of being robust to segmentation maps that result from splitting or merging segments of the ground truth [15, 16]. The PR index takes values between 0 and 1, with values closer to 0 (indicating an inferior segmentation result) and values closer to 1 (indicating a better result).

Fig. 1 shows the original Berkeley images used for the image segmentation experiment. These images with and without Gaussian noise are segmented by the proposed method, illustrated in Fig. 2. For fair comparison, we also evaluate the performance of GGFCM, FCM_S, FLICM and HMRF-FCM in addition to our methods. Table 1 presents the average PR values for all methods, corresponding to each of the test images in Fig. 1. Compared to other methods, the proposed algorithm yields the best segmentation results with the highest PR values.

Table 1. Comparison of different methods for Berkeley image dataset, Probabilistic Rand (PR) Index.

Image #	GGFCM	FCM_S	FLICM	HMRF-FCM	GFCM
135069	0.985	0.981	0.983	0.984	0.983
124084	0.708	0.510	0.510	0.526	0.732
69020	0.567	0.535	0.552	0.559	0.503
12003	0.622	0.608	0.614	0.618	0.630
58060	0.570	0.573	0.584	0.615	0.600
239007	0.665	0.633	0.645	0.668	0.660
46076	0.808	0.715	0.725	0.826	0.823
55067	0.887	0.879	0.879	0.888	0.889
353013+0.01noise	0.702	0.633	0.663	0.741	0.744
310007+0.01noise	0.620	0.664	0.708	0.677	0.705
61060+0.01noise	0.546	0.617	0.625	0.575	0.629
15088+0.02noise	0.698	0.656	0.717	0.855	0.861
24063+0.02noise	0.777	0.819	0.826	0.834	0.835
374067+0.02noise	0.695	0.711	0.729	0.744	0.778
302003+0.02noise	0.704	0.705	0.713	0.715	0.718
Mean	**0.704**	**0.683**	**0.698**	**0.722**	**0.739**

4.2. Multidimensional Images

In this experiment, we try to segment the multidimensional RGB color image into three classes: the blue sky, the red roof and the white wall. The original image (481×321) shown in Fig. 3(a) is corrupted by heavy Gaussian noise with mean=0 and covariance=0.15. The segmentation results of GGFCM, FCM_S, FLICM, HMRF-FCM and GFCM are shown in Figs. 3(b) through (f), respectively. The accuracy of segmentation for GGFCM is quite poor. This is expected that no spatial constraints are

taken into account in GGFCM. FCM_S, FLICM and HMRF-FCM obtain better results, but they are still sensitive to heavy noise. The accuracy of the segmentation results from GFCM, as shown in Fig. 3(f), is better than that of other methods, obtaining the highest PR values. It is worth pointing out that the PR value of HMRF-FCM (0.843) is just a little lower than the PR value of GFCM (0.849); however, the segmentation result of HMRF-FCM, shown in Fig. 3(e), is much poorer than GFCM (Fig. 3(f)).

We also evaluate the computation time for all methods in the previous experiment. The computation time t of the different methods is also presented in Fig. 3. It is noted that the computation of our methods is much faster than that of other methods. Compared to other methods, our model has the lowest computation burden and achieves the best segmentation results.

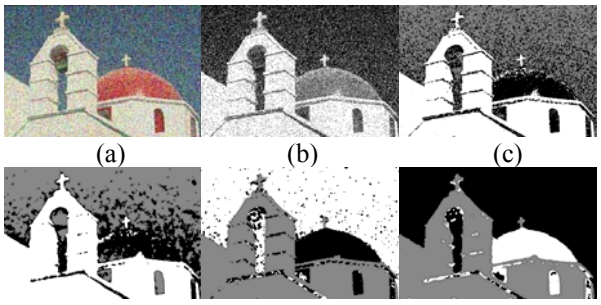

(a) (b) (c)

(d) (e) (f)

Fig. 3. Segment RGB Image with Gaussian noise. (a) Noised image (b) GGFCM, PR=0.667, t=9.28s (c) FCM_S, PR=0.759, t=4.23s (d) FLICM, PR=0.779, t=28.18s (e) HMRF-FCM, PR=0.843, t=167.53s (f) GFCM, PR=0.849, t=3.45s.

4.3. SAR Images

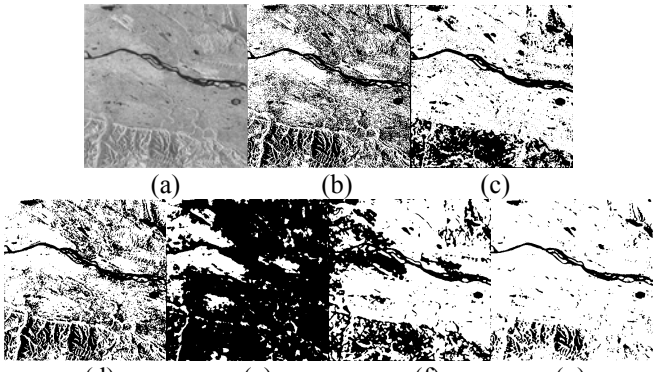

(a) (b) (c)

(d) (e) (f) (g)

Fig. 4. SAR Image Segmentation. (a) Original SAR image (b) GGFCM (c) MFCM (d) FCM_S (e) FLICM (f) HMRF-FCM (g) GFCM.

Synthetic aperture radar (SAR) data are often affected by speckle noise, which originates in the SAR system's coherent nature. In this experiment, we evaluate various methods based on real RADARSAT-1 SAR image. The original RADARSAT-1 SAR image (shown in Fig. 4(a)) represents a portion of the Northwest Territories (NWT) in Canada. With an area of 1,346,106 square kilometers, NWT is the largest region in the country after Nunavut. In the upper part of the image are the Franklin Mountains, and in the lower, the Mackenzie Mountains. These mountain ranges are separated by the Mackenzie River—the dark feature cutting across the middle of the image.

Our purpose is to distinguish the Mackenzie Mountains and the Mackenzie River. Thus we set the component number J=2. The segmentation results of GGFCM, MFCM, FCM_S, FLICM, HMRF-FCM and GFCM are shown in Figs. 4(b) through (g), respectively. Existence of noise has led to a "spotty" result using GGFCM and FCM_S shown in Fig. 4(b) and (d), respectively. FLICM and HMRF-FCM are failed to segment the SAR image, shown in Fig. 4(e) and (f), respectively. FLICM mixed the mountain and the river together and HMRF-FCM misclassifies some river parts. The MFCM shown in Fig. 4(c) gives an improved result; however, it loses some image details and is still not robust enough to image speckle. From Fig. 4(g), it can be seen that our GFCM obviously overcomes these shortcomings and preserve more details of mountain's ridges and river's tributaries. Through discussed above, we can conclude that the proposed GFCM is more robust to image speckle and can preserve more image details simultaneously.

5. CONCLUSION

In this paper, we propose a new simple and effective fuzzy clustering approach for image segmentation. The GFCM is introduced by incorporating the spatial constraints (generalized mean) into the fuzzy objective function. Although our algorithm is based on Euclidean distance, the distance function in FCM can be replaced by the general and flexible non-Euclidean function. In GFCM, the membership (or distance function) of an image pixel is influenced by the fuzzy membership (or distance function) of pixels in its immediate neighborhood with the help of the generalized mean. Different from the HMRF model, our model is fully free of any empirically adjusted parameters β and has less computation complexity. Compared with state-of-the-art technologies based on FCM, MFCM, HMRF and their hybrid models, the experimental results demonstrate the improved robustness and effectiveness of our proposed algorithm.

6. ACKOWLEDGEMENTS

This work was supported in part by the Canada Chair Research Program and the Natural Sciences and Engineering Research Council of Canada. This work was supported in part by the National Natural Science Foundation of China under Grant 61105007 and 61103141.

7. REFERENCES

[1] J. Yu, "General C-Means Clustering Model," IEEE Trans. Pattern Anal. Mach. Intell., vol. 27, no. 8, pp. 1197–1211, 2005.

[2] N. B. Karayiannis, "Weighted fuzzy learning vector quantization and weighted generalized fuzzy c-means algorithms," Proc. IEEE Conf. Fuzzy Systems, pp. 773–779, 1996.

[3] Krinidis S., and Chatzis V., "A Robust Fuzzy Local Information C-means Clustering Algorithm," IEEE Trans. Image Process., vol. 5, no. 19, pp. 1328–1337, 2010.

[4] M. Ahmed, S. Yamany, N. Mohamed, A. Farag, and T. Moriarty, "A Modified Fuzzy C-means Algorithm for Bias Field Estimation and Segmentation of MRI Data," IEEE Trans. Med. Imag., vol. 21, pp. 193–199, 2002.

[5] S. Chen and D. Zhang, "Robust Image Segmentation using FCM with Spatial Constraints based on new Kernel-induced Distance Measure," IEEE Transactions on Systems, Man and Cybernetics, vol. 34, no. 4, pp. 1907–1916, 2004.

[6] J. Bezdek, Pattern Recognition with Fuzzy Objective Function Algorithms. New York: Plenum, 1981.

[7] D. Pham and J.L. Prince, "An adaptive fuzzy c-means algorithm for image segmentation in the presence of intensity inhomogeneities," Pattern Recognit. Lett., vol. 20, pp. 57–68, 1999.

[8] Y.A. Tolias and S.M. Panas, "Image segmentation by a fuzzy clustering algorithm using adaptive spatially constrained membership functions," IEEE Trans. Syst., Man, Cybern. A, Syst. Humans, vol. 28, no. 3, pp. 359–369, 1998.

[9] S.P. Chatzis and T.A. Varvarigou, "A Fuzzy Clustering Approach Toward Hidden Markov Random Field Models for Enhanced Spatially Constrained Image Segmentation," IEEE Trans. Fuzzy Syst., vol. 16, no. 5, pp. 1351–1361, 2008.

[10] P. Clifford, "Markov Random Fields in Statistics," in Disorder in Physical Systems. A Volume in Honour of John M. Hammersley on the Occasion of His 70th Birthday, G. Grimmett and D. Welsh, Eds. Oxford, U.K.: Clarendon Press, Oxford Science Publication, 1990.

[11] L.R. Rabiner, "A Tutorial on Hidden Markov Models and Selected Applications in Speech Recognition," Proc. IEEE, vol. 77, no. 2, pp. 257-286, 1989.

[12] Y. Zhang, M. Brady, and S. Smith, "Segmentation of Brain MR Images Through a Hidden Markov Random Field Model and the Expectation Maximization Algorithm," IEEE Trans. Med. Imag., vol. 20, no. 1, pp. 45–57, 2001.

[13] J. Dunn, "A fuzzy relative of the ISODATA process and its use in detecting compact well separated clusters," Journal of Cybernetics, vol. 3, pp. 32–57, 1974.

[14] D. Martin, C. Fowlkes, D. Tal, and J. Malik, "A Database of Human Segmented Natural Images and its Application to Evaluating Segmentation Algorithms and Measuring Ecological Statistics," in Proc. 8th IEEE Int. Conf. Comput. Vis., Vancouver, BC, Canada, vol. 2, pp. 416–423, 2001.

[15] R. Unnikrishnan and M. Hebert, "Measures of Similarity," in Proc. IEEE Workshop Comput. Vis. Appl., pp. 394–400, 2005.

[16] Unnikrishnan R., Pantofaru C., and Hebert M., "A Measure for Objective Evaluation of Image Segmentation Algorithms," IEEE Conf. Comput. Vis. Pattern Recognit., vol. 3, pp. 34–41, 2005.